

Identifying the critical point of the weakly first-order itinerant magnet DyCo₂ with complementary magnetization and calorimetric measurements

K. Morrison,^{1,3} A. Dupas,¹ Y. Mudryk,² V. K. Pecharsky,² K. A. Gschneidner,² A. D. Caplin,¹ and L. F. Cohen¹

¹*The Blackett Laboratory, Imperial College, London SW7 2BZ, UK*

²*Ames Laboratory, U.S. Department of Energy and Department of Materials Science and Engineering, Iowa State University, Ames, Iowa, 50011-3020, USA*

³*Department of Physics, Loughborough University, Loughborough, LE11 3TU, UK*

(Received 31 May 2012; published 25 April 2013)

We examine the character of the itinerant magnetic transition of DyCo₂ by different calorimetric methods, thereby separating the heat capacity and latent heat contributions to the entropy—allowing direct comparison to other itinerant electron metamagnetic systems. The heat capacity exhibits a large λ -like peak at the ferrimagnetic ordering phase transition, a signature that is remarkably similar to La(Fe,Si)₁₃, where it is attributed to giant spin fluctuations. Using calorimetric measurements, we also determine the point at which the phase transition ceases to be first order: the critical magnetic field, $\mu_0 H_{\text{crit}} = 0.4 \pm 0.1$ T and temperature $T_{\text{crit}} = 138.5 \pm 0.5$ K, and we compare these values to those obtained from analysis of magnetization by application of the Shimizu inequality for itinerant electron metamagnetism. Good agreement is found between these independent measurements, thus establishing the phase diagram and critical point with some confidence. In addition, we find that the often-used Banerjee criterion may not be suitable for determination of first order behavior in itinerant magnet systems.

DOI: [10.1103/PhysRevB.87.134421](https://doi.org/10.1103/PhysRevB.87.134421)

PACS number(s): 75.30.Sg, 75.30.Kz, 75.40.-s, 75.50.Cc

I. INTRODUCTION

With recent interest in first order magnetic phase transitions for room-temperature refrigeration,^{1–3} certain classes of materials have generated much attention. In particular, the cubic NaZn₁₃-type La(Fe,Si)₁₃ (Ref. 4) and the hexagonal Fe₂P-type Mn_xFe_{1.95–x}P_{1–y}Si_y (Ref. 5)—both of which are itinerant electron metamagnets (IEM)—show significant promise. La(Fe,Si)₁₃ has a giant entropy change with large associated latent heat and a signature giant λ -like heat capacity at the transition,^{6–8} whereas Mn_xFe_{1.95–x}P_{1–y}Si_y has been much less studied. The study of these systems reinvigorates an interest in IEM systems and in particular the nature of the transition and how it evolves in applied magnetic field—all important for magnetocaloric applications.

Here, RCo₂ (where R is the rare-earth element) is a well-established IEM system.⁹ The choice of R affects the lattice parameter, and as a result the bulk magnetic behavior via $4f$ - $3d$ exchange.¹⁰ Furthermore, the lattice parameter a can be tuned such that a small change in applied field, temperature, and/or pressure can induce magnetic order ($7.05 \text{ \AA} < a < 7.22 \text{ \AA}$),^{6,11} and an associated volume change (or distortion) occurs to reduce the increase in energy due to overlap of $3d$ bands. If that volume change is sufficiently large, the phase transition will be first order,¹² and itinerant electron metamagnetism occurs.¹³

In DyCo₂—an IEM of potential interest for low-temperature magnetocaloric applications¹⁴—a first order phase transition was predicted^{13,15} and observed by x-ray diffraction (XRD) in zero field, where a cubic-tetragonal distortion occurs alongside the magnetic transition^{16,17} (these same XRD measurements showed that, in a magnetic field of 4 T, the phase transition is continuous). Nevertheless, in spite of the extensive work on this system, the details of the magnetic field–temperature (H - T) phase diagram are much less established, and the critical point (where the

first order transition disappears) has not previously been determined.^{18–20}

Here, we study DyCo₂ using both magnetic and calorimetric methods to investigate whether there is a giant enhancement of the heat capacity C_p close to T_c as previously observed in the La(Fe,Si)₁₃ system.^{6,7} We obtain the latent heat and C_p separately, so that we can also establish the relationship between latent heat and hysteresis in this system. We find that both vanish at a critical point which we establish in the H - T phase diagram. We also employ the Shimizu inequality (derived from spin fluctuation theory)^{21,22} that defines the onset of IEM to determine the field H_{crit} and temperature T_{crit} of the critical point. Finally, we discuss the validity of the Shimizu inequality compared to the widely used Banerjee criterion²³ for determination of the onset of first order behavior.

One technical complication is that, often, it is difficult experimentally to distinguish a latent heat from a rapidly varying heat capacity, as will be discussed in detail below. For consistency in nomenclature, we refer to the true heat capacity always as C_p and in any measurement that may include a latent heat contribution as “total heat capacity”.

II. EXPERIMENTAL DETAILS

The DyCo₂ alloy was prepared by arc melting the pure metals under purified argon atmosphere. Dysprosium was obtained from the Materials Preparation Center²⁴ of Ames Laboratory of the U.S. Department of Energy, and major impurities (in atomic parts per million) were O = 1190 and C = 459. Cobalt was purchased from Johnson Matthey Chemicals Limited (Alfa Aesar) and was 99.95 at.% pure. A small amount (2 at.%) of Dy has been added in excess to the stoichiometrically calculated Dy:Co ratio in order to (1) compensate for the weight loss of Dy during arc melting and (2) prevent the formation of the congruently melting DyCo₃

phase (a common impurity in DyCo₂, which forms from DyCo₃ and liquid by a peritectic reaction). An ~8-g button was remelted three times and then broken into a few pieces. The heat treatment was performed in a sealed quartz ampoule filled with inert gas at 1173 K for 5 d. Phase purity of the material was checked by x-ray powder diffraction analyses followed by Rietveld refinement of the x-ray diffraction patterns. X-ray analyses of the heat-treated sample revealed no detectible impurities (within the 2% sensitivity of the x-ray powder diffraction method).

Magnetization measurements on approximately 40 mg quasispherical samples, hereafter referred to as “bulk”, were carried out in a Quantum Design vibrating sample magnetometer (VSM) for temperatures ranging from 100–240 K and at field sweep rates of 0.5 T/min. Slower field sweep rates close to T_c (where the field hysteresis, $H_c^\uparrow - H_c^\downarrow$, is larger) confirmed that any hysteresis seen was intrinsic to the material system and not a result of nonisothermal conditions due to the magnetocaloric effect itself.²⁵ The magnetic data were corrected for demagnetization effects with a demagnetization factor $N = 0.33$.

Microcalorimetry measurements were performed on a 100- μm fragment taken from the bulk sample ($m = 2.6 \pm 0.2 \mu\text{g}$) using a commercial Xensor (TCG-3880) SiN membrane chip adapted to work either as an ac calorimeter²⁶ or as an adiabatic temperature probe^{27,28} in a cryostat capable of $B = 0\text{--}8$ T, $T = 5\text{--}295$ K.

When operated as an ac calorimeter, as described by Minakov *et al.*,²⁶ an ac temperature modulation (heating) is applied to a sample held in an exchange gas of He. The sample size is limited to the size of the heater area ~100 μm , corresponding to a typical sample mass of a few micrograms. Thermopile junctions located at the sample and 1 mm away (~ T_{bath}) measure the phase and amplitude of the resultant thermal modulation with respect to the source signal; the solution of the heat transfer equation yields the heat capacity C_p . As the ac measurement is a modulation technique, it measures C_p alone and does not measure the latent heat L .⁸ Any latent heat that may occur on first driving the phase transition will be neither repeatable nor reversible on subsequent ac cycles, within the limitations of the technique as described in depth in Ref. 8.

When operated as an adiabatic temperature probe, as outlined by Miyoshi *et al.*,²⁷ the He exchange gas is pumped out (to $P < 5 \times 10^{-2}$ mbar), and a passive measurement of the temperature change in response to an applied magnetic field (typically swept at a rate of 0.5 T/min) is obtained. For a sharp first order transition, the latent heat appears as a spiked peak as the field passes through the onset field H_c .^{7,27,29} This peak will have a characteristic decay time of ~1 s. For polycrystalline samples with a correlation length (measure of the nucleation volume) of less than 100 μm the transition will manifest as a series of spikes distributed in field as successive regions undergo the transition. The noise floor of this measurement is of the order of 1 μV , equivalent to ~10 nJ.

Zero-field (relaxation type) heat capacity measurements were carried out on a larger, polished bulk sample ($m = 12.5 \pm 0.1$ mg) using a Quantum Design Physical Property Measurement System (PPMS) as a secondary check of the absolute magnitude of C_p . The scanning method outlined by

Lashley *et al.*³⁰ and Suzuki *et al.*³¹ was employed to resolve the peak in the total heat capacity at T_c .

III. INDIRECT DETERMINATION OF LATENT HEAT

For first order phase transitions where the nucleation volume is less than 100 μm , the latent heat response measured by the microcalorimeter becomes distributed in temperature (or field), and so can fall below the resolution of the adiabatic temperature probe. We have established that, in these circumstances, L can be estimated indirectly from ac calorimetric measurements of C_p (the true heat capacity) by careful accounting of entropy changes.²⁸

The contribution of C_p to the total entropy change, $\Delta S_{HC}(T^*)$, on increasing the field from H_1 to H_2 at temperature T^* can be written as:²⁸

$$\begin{aligned} \Delta S_{HC}(T^*)_{\Delta H} &= \Delta S(T_{\text{ref}})_{\Delta H} \\ &+ \int_{T_{\text{ref}}}^{T^*} \frac{C_p(H_2, T) - C_p(H_1, T)}{T} dT \\ &- \left[\frac{L(H_1)}{T_c(H_1)} - \frac{L(H_2)}{T_c(H_2)} \right] \Big|_{T^* < T_c(H_1)}, \quad (1) \end{aligned}$$

$$\begin{aligned} \Delta S_{HC}(T^*)_{\Delta H} &= \Delta S(T_{\text{ref}})_{\Delta H} \\ &+ \int_{T_{\text{ref}}}^{T^*} \frac{C_p(H_2, T) - C_p(H_1, T)}{T} dT \\ &- \left[\frac{L(T)}{T} - \frac{L(H_2)}{T_c(H_2)} \right] \Big|_{T^* > T_c(H_1)}, \quad (2) \end{aligned}$$

where ΔH is the chosen field change ($= H_2 - H_1$), and $L(H_x)$ is the latent heat at field H_x with corresponding transition temperature $T(H_x)$. These equations consist of three terms: The integration constant $\Delta S(T_{\text{ref}})$; the integral $\int (\Delta C/T) dt$; and a correction term $K(H_1, H_2)$ due to any latent heat $[L(H, T)]$ that varies with temperature. The limit of integration T_{ref} is a temperature chosen so that the thermodynamic properties are only weakly temperature dependent [i.e. $\Delta S(T_{\text{ref}})$ is small]; T_{ref} was taken as 220 K here.

To determine the correction term K due to temperature-dependent L , we compare ΔS_{HC} measured below T_c with ΔS_{Max} , the entropy change obtained from magnetometry measurements using the Maxwell relation (while being careful to avoid the integration artifacts due to a first order phase transition).³²

For the case $T_{\text{ref}} > T_c$, by rearranging Eq. (1) and setting $\Delta S_{\text{Max}} = \Delta S_{HC}$ for T_{comp} (where T_{comp} is a temperature chosen for the comparison such that $T_{\text{comp}} \ll T_c$ and taken here as 110 K), the offset between the two measurements, denoted here as $K(H_1, H_2)$, is found, as described by Eq. (3):

$$\begin{aligned} K(H_1, H_2) &= \left[\Delta S(T_{\text{ref}})_{\Delta H} + \int_{T_{\text{ref}}}^{T_{\text{comp}}} \frac{C_p(H_2, T) - C_p(H_1, T)}{T} dT \right] \\ &- \Delta S_{\text{Max}}(T_{\text{comp}})_{\Delta H} = \frac{L(H_1)}{T_c(H_1)} - \frac{L(H_2)}{T_c(H_2)}. \quad (3) \end{aligned}$$

Notice that Eq. (3) describes the difference in latent heat at fields H_1 and H_2 . This can be used to estimate the latent heat contribution, and we have previously demonstrated the validity of the correction process in a first order manganite

with a distributed ΔS_L caused by a high variability in the occupation of the A site.²⁸ The strength of this technique is that: (1) one can determine $\Delta S_L(0\text{ T})$ where it might otherwise be uncertain; (2) it can be used to determine H_{crit} accurately; and (3) it demonstrates explicitly whether a phase transition is first order or not.

IV. IDENTIFYING THE CRITICAL POINT

A. Calorimetric method

The zero-field phase transition of DyCo_2 is first order.⁹ In order to quantify this, we first measured C_p using the ac calorimetry probe. The results are shown in the main panel of Fig. 1. We stress again that the ac technique employed does not sample L directly and have demonstrated this for several systems previously.^{8,28,29} The first observation is that the signature enhancement of C_p of the order of 600% is similar to that seen in the $\text{La}(\text{Fe}_{1-x}\text{Si}_x)_{13}$ material system,⁶ and it is quickly suppressed when the magnetic field and temperature are increased. In contrast, Gd (a local moment system which undergoes a continuous phase transition) also shows a large λ -like change in C_p , but of the order of 100% only.³³ CoMnSi (which is also thought to be a local moment system that undergoes a first order magnetoelectric phase transition) shows a change of C_p at the antiferromagnetic/ferromagnetic (AFM/FM) transition of only 5%, accompanied by a large latent heat.²⁹ So it is reasonable to describe the change in C_p in DyCo_2 as giant, and it is interesting that it is similar in magnitude to a previously studied IEM system: $\text{La}(\text{Fe}_{1-x}\text{Si}_x)_{13}$.^{6,8}

The latent heat as measured by the adiabatic probe approaches the limit of its resolution.²⁸ The left-hand inset to Fig. 1 shows raw data from the adiabatic temperature probe run at 137.2 K where the heat capacity peak was at its maximum. Although the signal is weak and distributed, it does indicate the presence of a latent heat, supporting the known first order nature of the transition. The temperature dependence of C_p also indicates first order behavior: The right-hand inset of Fig. 1 shows the S - T plot determined by integrating the total heat capacity (C_{total}/T) from 10 K. By comparing the change

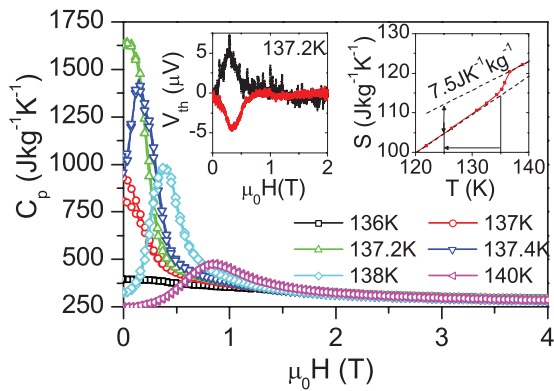


FIG. 1. (Color online) Heat capacity as a function of field at selected temperatures about T_c for both field increase and decrease; $C_{\text{peak}} \sim 1650 \text{ Jkg}^{-1}\text{K}^{-1}$ at $T = 137.2 \text{ K}$, $\mu_0 H = 0 \text{ T}$, almost 7 times larger than $C_p(T > T_c)$. Inset left: Signature of distributed latent heat measured at 137.2 K. Inset right: S - T plot determined by integrating the zero-field total heat capacity from 10 K.

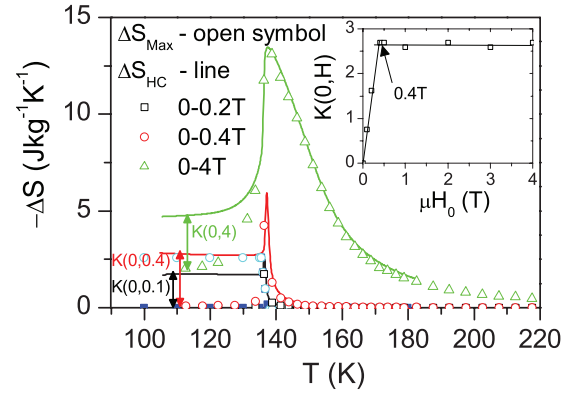


FIG. 2. (Color online) Entropy change ΔS_{HC} calculated by integrating C_p from $T_{\text{ref}} = 220 \text{ K}$. The offset in ΔS_{HC} compared to ΔS_{Max} below T_c ($\sim 135 \text{ K}$), is an indication of the temperature dependent latent heat ΔS_L . Inset shows this offset $K(0, H)$ (in same units, $\text{Jkg}^{-1}\text{K}^{-1}$) plotted as a function of the critical field and indicates $\Delta S_L(0\text{ T}) = 2.6 \pm 0.5 \text{ Jkg}^{-1}\text{K}^{-1}$.

in entropy S from 10 K below T_c to just above T_c , the total entropy change in zero field is estimated to be $\Delta S(0\text{ T}) \sim 7.5 \text{ Jkg}^{-1}\text{K}^{-1}$, which is of a similar magnitude to previously reported values.^{18,34,35} The change in entropy obtained in this way from C_p alone is $\Delta S_{HC}(0\text{ T}) = 5 \pm 0.2 \text{ Jkg}^{-1}\text{K}^{-1}$. These two measurements suggest that the latent heat contribution to the entropy change at the transition is of the order of $2.5 \text{ Jkg}^{-1}\text{K}^{-1}$, which is significant.

To determine the latent heat contribution to the total entropy change in 0 T explicitly, we first consider the measurement of C_p in detail, as shown in Fig. 2 where the calculated values of ΔS_{HC} alongside ΔS_{Max} are plotted for several field changes before the correction term $K(H_1, H_2)$ [defined in Eq. (3)] is applied. As stated previously, the correction term $K(H_1, H_2)$ is a consequence of temperature-dependent latent heat on the integration of C_p .²⁸ Thus, the derived values of $K(0, H)$ which saturate for $H > 0.4 \text{ T}$ (as shown in the inset of Fig. 2) indicate a clearly defined critical field $H_{\text{crit}} = 0.4 \text{ T}$ where the phase transition changes from first order to continuous. From this, the zero-field latent heat contribution to the total entropy change was determined as $\Delta S_L(0\text{ T}) = 2.6 \pm 0.5 \text{ Jkg}^{-1}\text{K}^{-1}$. Notice that the sum of $\Delta S_{HC}(0\text{ T})$ and $\Delta S_L(0\text{ T})$ is in agreement (within error) with the total zero-field entropy change $\Delta S(0\text{ T})$ of $7.5 \text{ Jkg}^{-1}\text{K}^{-1}$ observed here and elsewhere.^{18,34,35}

Herein lies the strength of this technique: Not only can we measure ΔS_{OT} , as is often cited in literature, but we can also separate it into the latent heat expelled at the phase transition and the continuous change in heat capacity. This analysis can provide insight into the evolution of these two contributions as we approach a critical point and also allows direct comparison between the magnitude of L and the size of the associated field (or thermal) hysteresis.

B. Magnetization method

In 1964, Banerjee put forward a “generalized approach to first and continuous magnetic transitions”.²³ He outlined a criterion to distinguish a magnetic transition as first order or continuous from magnetic data alone by combining the Bean–Rodbell model¹² with the Landau–Lifshitz

thermodynamic theory of continuous phase transitions. The free energy expansion is given in Eq. (4), where H is the applied field and M the magnetization. At T_c , $dF/dM = 0$, thus by differentiating Eq. (4) with respect to M and rearranging, we obtain Eq. (5):

$$F = A/2M^2 + B/4M^4 + C/6M^6 + D/8M^8 + \dots - HM, \quad (4)$$

$$H/M = A + BM^2 + CM^4 + DM^6 + \dots \quad (5)$$

The Banerjee criterion assumes that the higher-order terms in Eq. (4) can be ignored, which is a reasonable assumption at low M^2 ; thus, the coefficients C and D in Eqs. (4) and (5) are set as zero. It follows that, if the value of B , defined in Eq. (5), is negative, the phase transition is first order. It also follows that larger values of $|B|$ indicate a larger energy barrier and thus a stronger first order phase transition. However, this criterion is widely used even though it is difficult to implement correctly for weakly or disordered first order systems in general (where B is either very small or influenced by disorder broadening of the T_c) and inaccurate for itinerant systems such as DyCo_2 in particular (where spin fluctuations not considered in the mean field model should be taken into account).

As the mean field approximation (used in the Banerjee criterion and the Bean–Rodbell model¹²), does not allow for fluctuations of moments about their equilibrium values, an additional correction is required for itinerant systems. For example, as the temperature is increased, spin fluctuations act to lower (renormalize) the energy barrier, separating two metastable states,³⁶ which has the impact of driving a weakly first order phase transition (small, but negative B) towards a continuous phase transition. These fluctuations underpin the free energy inequality derived for IEM by Shimizu *et al.*^{21,22,37}

$$3/16 < AC/B^2 < 9/20. \quad (6)$$

When this inequality is satisfied and $A > 0$, $C > 0$, and $B < 0$, a stable (first order) IEM transition can occur.

Figure 3 shows that the higher-order terms in Eq. (5) are required to fit the full curve (where the values of A and B were fixed at low M^2 values to minimize the number of free parameters in the fitting routine). We note that for any S -shaped M - H curves, phenomenological fitting to the second

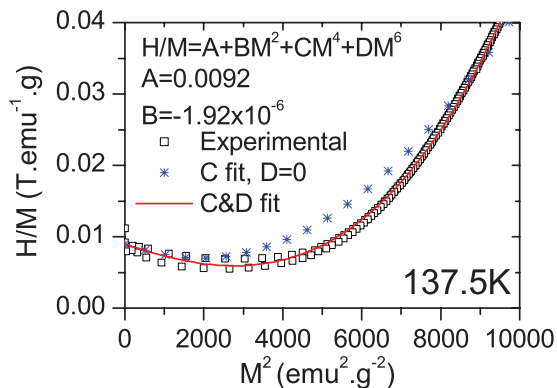


FIG. 3. (Color online) Landau fit at 137.5 K for DyCo_2 where parameters A and B , as defined in the text, are fixed at values determined as M^2 approaches zero. Similarly poor fits were observed for other temperatures ($T > T_c$) when parameter D was set to zero.

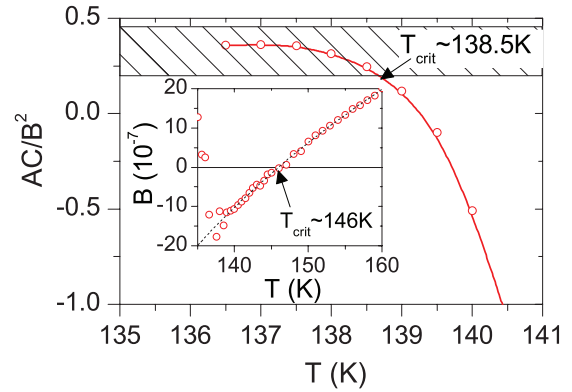


FIG. 4. (Color online) Stability of itinerant metamagnetic behavior as a function of temperature. The hashed area indicates possible values for stable first order IEM as defined by the Shimizu inequality given in the text. The data shown here indicates $T_{\text{crit}} \sim 138.5$ K. Inset shows the value of B as a function of temperature where $B < 0$ for $T < 146$ K, indicating by the Banerjee criterion that $T_{\text{crit}} < 146$ K.

coefficient B alone will never yield a good fit. To determine the value of C for use in the inequality of Eq. (6), A and B were fixed to their values at low M^2 (as for Fig. 3), leaving C and D as free parameters in the fit following Eq. (5). Figure 4 shows the resultant values of AC/B^2 plotted as a function of temperature, with the shaded area indicating the region described by the Shimizu inequality of Eq. (6). From this, we obtain $T_{\text{crit}} = 138.5 \pm 0.5$ K. The inset of Fig. 4 shows the temperature dependence of B , where the often-used Banerjee criterion yields $T_{\text{crit}} < 146$ K.

V. DETERMINING THE PHASE DIAGRAM FROM HEAT CAPACITY AND MAGNETIZATION DATA

So far, we have determined $T_{\text{crit}} = 138.5 \pm 0.5$ K from applying the Shimizu criterion to magnetization data and $\mu_0 H_{\text{crit}} = 0.4 \pm 0.1$ T from the vanishing of L in microcalorimetric data. There could be some difference between bulk and fragment data, as the former incorporates a distribution of T_c , but the latter may have only a smaller subset of this distribution. This usually happens in the systems that are nonstoichiometric, in which compositional gradients may occur at different length scales. Since DyCo_2 is a stoichiometric compound, it is most likely that a small fragment should remain representative of the bulk. There might also be a strain relief in the system by the process of fragmentation.^{38,39} To check whether bulk and fragment differ, we measured M - H loops of a collection of fragments ($< 100 \mu\text{m}$) and compared them to the bulk, as can be seen in Fig. 5(a). As expected, there is neither a shift in the critical field H_c nor a decrease in the hysteresis ΔH , in contrast to other systems where compositional inhomogeneities, poor thermal conductivity, and/or strong magnetostructural coupling (strain relief) play a role.^{25,39} As such, it seems our estimates of T_{crit} and H_{crit} are valid for both bulk and fragmented samples.

Figure 5(a) also shows the critical field H_c , determined from the midpoint of the bulk M - H loops, where $M = M_{PM} + (M_{PM} - M_{FM})/2$, M_{PM} is the moment of the paramagnetic (PM) phase, and M_{FM} is the moment of the FM phase at H_c . The phase diagram determined this way is given in Fig. 5(b).

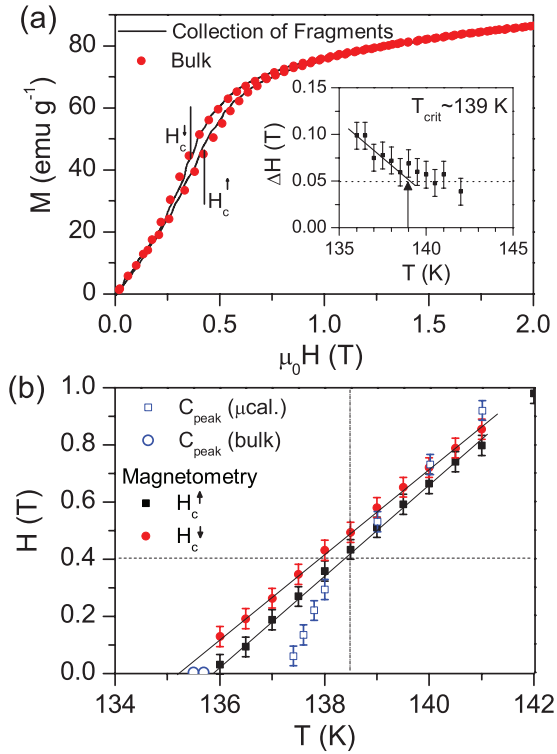


FIG. 5. (Color online) (a) Example bulk and fragment M - H loop at 138 K. Inset shows hysteresis ($\Delta H = H_c^\uparrow - H_c^\downarrow$) as a function of temperature where the 0.05 T is a minimum baseline due to experimental artifacts. (b) Critical field H_c determined from bulk magnetometry and position of the heat capacity peak C_{peak} from bulk and microcalorimetry data. The position of the ac heat capacity peak is the same (within symbol size) for field increase and decrease (as shown in Fig. 1). The dashed lines indicate the T_{crit} and H_{crit} as determined by magnetometry and calorimetry, respectively. The field and temperature at which hysteresis approaches zero [see inset of (a)] and C_{peak} approaches the bulk phase line corresponds to $H_{\text{crit}} = 0.45$ T and $T_{\text{crit}} = 138.5$ K.

Note that the uncertainty in $\mu_0 H_c$ is limited to 0.035 T by both the time constant of the lock-in used and the chosen field sweep rate and will increase as the M - H loop broadens, as is indicated by the error bars of Fig. 5(b). The inset of Fig. 5(a) shows the hysteresis $\Delta H = H_c^\uparrow - H_c^\downarrow$ determined from these critical fields with a combined error producing a baseline as indicated of 0.05 T.

Also shown in Fig. 5(b) is the trajectory of the peak in C_p measured by ac calorimetry C_{peak} . The subtlety of the field dependence of C_{peak} is that it approaches the magnetically determined phase line as the first order behavior vanishes, determined here as $T_{\text{crit}} = 138.5$ K. These observations indicate that the magnetic behavior of DyCo_2 is consistent with the Shimizu inequality, as expected for an itinerant system.

VI. DISCUSSION

It is important to compare our results to those found in the literature. As previously mentioned, the Bean–Rodbell model is a mean field (approximation) method that describes the relationship between the volume change and order of the phase transition based on magnetoelastic coupling in the system.¹²

One outcome of this model is the quantity η :

$$\eta = \frac{40Nk_B\kappa T_0\beta^2 j^2(j+1)^2}{(2j+1)^4 - 1}, \quad (7)$$

where j is the spin quantum number ($= 0.5$ for Co and 5 for Dy); $\beta = (T_c/T_o - 1)[V_o/(V - V_o)]$ and T_o and V_o are the Curie temperature and the volume in the absence of an exchange interaction, respectively. κ is the isothermal compressibility; and N is the number of magnetic carriers per unit volume. If $\eta > 1$, then the phase transition is considered first order by this model. For example, the model was applied to the ideal $\text{La}(\text{Fe},\text{Si})_{13}$ system to demonstrate the relationship between volume change at the transition and magnetic exchange.⁴⁰ The $\text{La}(\text{Fe},\text{Si})_{13}$ system is ideal because, at the phase transition, there is a volume expansion of the cubic lattice (no change of symmetry), and the only contribution to the total magnetic moment comes from the Fe atoms ($2 \mu_B$ per Fe atom). By substituting Si for Fe, the phase transition is driven from first order to continuous, and it was shown by application of this model that a continuous phase transition could still exist when accompanied by some volume change.⁴⁰ Unfortunately, such a simple comparison is not possible for DyCo_2 as: (a) The system is composed of two sublattices of Dy and Co acting in opposition (ferrimagnet); and (b) a cubic-tetragonal distortion occurs at the phase transition, with opposing changes in the lattice parameters a and c resulting overall in a lower volume change.¹⁷ Clearly, the Bean–Rodbell model is not readily applicable to this system, so we instead formulate a qualitative assessment of its behavior.

The in-field XRD measurements presented by Pecharsky *et al.*¹⁷ showed a clear discontinuity in the lattice parameters at T_c ($H = 0$ T), which indicates first order character, whereas by 4 T, the volume change was observed to be continuous with temperature. These observations are consistent with magnetostriction data (for fields as high as 15 T) that indicated that the field-driven lattice distortion persists to high fields.⁴¹

Herrero *et al.*¹⁸ used differential scanning calorimetry (DSC) to examine the magnetic phase transitions in a number of $R\text{Co}_2$ compounds. For DyCo_2 , they report a large peak in the DSC scans that persists in magnetic fields of up to 1.5 T; they attributed this peak to the latent heat associated with a first order transition, despite commenting that they see no indication of any hysteresis. The apparent discrepancy between our two reports lies, however, in the interpretation of the term “latent heat.” Where we separate large background changes in the heat capacity across the transition (from a latent heat associated with a hysteretic process), DSC is incapable of distinguishing a peak in the heat capacity—as is often present at continuous phase transitions—from a true latent heat (indicative of a first order transition). Consequently, the DSC measurements provide no evidence of the first order transition in DyCo_2 persisting above the critical field of 0.4 T that we infer.

VII. CONCLUSION

Here, we confirm explicitly that in zero field, the Laves phase compound DyCo_2 exhibits a first order phase transition, but it is quickly suppressed by applied field.¹⁷ Using a newly developed extension of the microcalorimetry technique in conjunction with magnetic data and the Maxwell relation,

we estimate the zero-field latent heat contribution [to the total $\Delta S(0\text{ T}) = 7.5\text{ Jkg}^{-1}\text{K}^{-1}$] of $\Delta S_L(0\text{ T}) = 2.6 \pm 0.5\text{ Jkg}^{-1}\text{K}^{-1}$, and the field above which $\Delta S_L = 0$ as $\mu_0 H_{\text{crit}} = 0.4 \pm 0.1\text{ T}$, corresponding to $T_{\text{crit}} = 138.5 \pm 0.5\text{ K}$. These critical field and temperature values are consistent with those extracted from independent magnetization data using the Shimizu criterion, thus defining the critical parameters conclusively. We also note a striking similarity between DyCo_2 and the itinerant system $\text{La}(\text{Fe},\text{Si})_{13}$, where although the latent heat is a significant fraction of the total entropy change, the hysteresis is still relatively low and that both systems show a large and characteristic enhancement of C_p , which may be associated with the spin fluctuation contribution at the transition.

ACKNOWLEDGMENTS

The research leading to these results has received funding from the European Community's 7th Framework Programme under Grant Agreement No. 214864 ("SSEEC") and EPSRC EP/G060940/1. The sample preparation and x-ray characterization were performed at the Ames Laboratory of the U.S. Department of Energy. Work at Ames Laboratory is supported by the Office of Basic Energy Sciences, Materials Sciences Division of the Office of Science, U.S. Department of Energy. The Ames Laboratory is operated by Iowa State University of Science and Technology for the U.S. Department of Energy under Contract No. DE-AC02-07CH11358.

- ¹A. M. Tishin and Y. I. Spichkin, *The Magnetocaloric Effect and its Applications* (IOP Publishing Ltd., Bristol, Philadelphia, 2003).
- ²V. K. Pecharsky and K. A. Gschneidner, *Phys. Rev. Lett.* **78**, 4494 (1997).
- ³V. K. Pecharsky and K. A. Gschneidner, *Adv. Mater.* **13**, 683 (2001).
- ⁴O. Gutfleisch, M. Willard, E. Brück, C. Chen, S. Sankar, and J. Liu, *Adv. Mater.* **23**, 821 (2011).
- ⁵H. D. Nguyen, O. Zhi Qiang, C. Luana, Z. Lian, T. C. T. Dinh, A. d. W. Gilles, A. d. G. Rob, K. H. J. Buschow, and B. Ekkes, *Advanced Energy Materials* **1**, 1215 (2011).
- ⁶K. Morrison, S. M. Podgornykh, Ye. V. Shcherbakova, A. D. Caplin, and L. F. Cohen, *Phys. Rev. B* **83**, 144415 (2011).
- ⁷K. Morrison, J. Lyubina, J. D. Moore, A. D. Caplin, K. G. Sandeman, O. Gutfleisch, and L. F. Cohen, *J. Phys. D: Appl. Phys.* **43**, 132001 (2010).
- ⁸K. Morrison, J. Lyubina, J. D. Moore, K. G. Sandeman, O. Gutfleisch, L. F. Cohen, and A. D. Caplin, *Philos. Mag.* **92**, 1 (2012).
- ⁹S. Khmelevskiy and P. Mohn, *J. Phys.: Condens. Matter.* **12**, 9453 (2000).
- ¹⁰H. R. Kirchmayr and C. A. Poldy, *J. Magn. Magn. Mater.* **8**, 1 (1978).
- ¹¹Z. Arnold, C. Magen, L. Morellon, P. A. Algarabel, J. Kamarad, M. R. Ibarra, V. K. Pecharsky, and K. A. Gschneidner, *Phys. Rev. B* **79**, 144430 (2009).
- ¹²C. P. Bean and D. S. Rodbell, *Phys. Rev.* **126**, 104 (1962).
- ¹³N. Singh, K. Suresh, A. Nigam, and S. Malik, *J. Magn. Magn. Mater.* **317**, 68 (2007).
- ¹⁴N. H. Duc, D. T. K. Anh, and P. E. Brommer, *Physica B: Condensed Matter* **319**, 1 (2002).
- ¹⁵E. Gratz, R. Resel, A. T. Burkov, E. Bauer, A. S. Markosyan, and A. Galatanu, *J. Phys.: Condens. Matter.* **7**, 6687 (1995).
- ¹⁶V. K. Pecharsky, Ya. Mudryk, and K. A. Gschneidner, Jr., *Z. Kristallogr. Suppl.* **26**, 139 (2007).
- ¹⁷V. K. Pecharsky, K. A. Gschneidner, Jr., Ya. Mudryk, and Durga Paudyal, *J. Magn. Magn. Mater.* **321**, 3541 (2009).
- ¹⁸J. Herrero-Albillos, F. Bartolomé, L. M. García, F. Casanova, A. Labarta, and X. Batlle, *Phys. Rev. B* **73**, 134410 (2006).
- ¹⁹M. Parra-Borderías, F. Bartolomé, J. Herrero-Albillos, and L. M. García, *J. Alloys Compd.* **481**, 48 (2009).
- ²⁰C. M. Bonilla, J. Herrero-Albillos, F. Bartolomé, L. M. Garcia, M. Parra-Borderías, and V. Franco, *Phys. Rev. B* **81**, 224424 (2010).
- ²¹M. Shimizu, *Proc. Phys. Soc.* **84**, 397 (1964).
- ²²M. Shimizu, *Proc. Phys. Soc.* **86**, 147 (1965).
- ²³S. K. Banerjee, *Phys. Lett.* **12**, 16 (1964).
- ²⁴Materials Preparation Center, Ames Laboratory of U.S. Department of Energy, Ames, IA, [www.mpc.ameslab.gov].
- ²⁵J. D. Moore, K. Morrison, K. G. Sandeman, M. Katter, and L. F. Cohen, *Appl. Phys. Lett.* **95**, 252504 (2009).
- ²⁶A. A. Minakov, S. B. Roy, Y. V. Bugoslavsky, and L. F. Cohen, *Rev. Sci. Instrum.* **76**, 043906 (2005).
- ²⁷Y. Miyoshi, K. Morrison, J. D. Moore, A. D. Caplin, and L. F. Cohen, *Rev. Sci. Instrum.* **79**, 074901 (2008).
- ²⁸K. Morrison, M. Bratko, J. Turcaud, A. Berenov, A. D. Caplin, and L. F. Cohen, *Rev. Sci. Instrum.* **83**, 033901 (2012).
- ²⁹K. Morrison, A. Barcza, J. D. Moore, K. G. Sandeman, M. K. Chattopadhyay, S. B. Roy, A. D. Caplin, and L. F. Cohen, *J. Phys. D: Appl. Phys.* **43**, 195001 (2010).
- ³⁰J. C. Lashley, M. F. Hundley, A. Migliori, J. L. Sarrao, P. G. Pagliuso, T. W. Darling, M. Jaime, J. C. Cooley, W. L. Hults, L. Morales, D. J. Thoma, J. L. Smith, J. Boerio-Goates, B. F. Woodfield, G. R. Stewart, R. A. Fisher, and N. E. Phillips, *Cryogenics* **43**, 369 (2003).
- ³¹H. Suzuki, A. Inaba and C. Meingast, *Cryogenics* **50**, 693 (2010).
- ³²L. Caron, Z. Q. Ou, T. T. Nguyen, D. T. Cam Thanh, O. Tegus, and E. Brück, *J. Magn. Magn. Mater.* **321**, 3559 (2009).
- ³³S. Y. Dan'kov, A. M. Tishin, V. K. Pecharsky, and K. A. Gschneidner, Jr., *Phys. Rev. B* **57**, 3478 (1998).
- ³⁴Y. Mudryk, V. K. Pecharsky, and K. A. Gschneidner, Jr., in *Proceedings of the 3rd IIF-IIR International Conference Magnetic Refrigeration at Room Temperature, Des Moines, Iowa USA, 2009*, edited by P. Egolf (Institut International du Froid, Paris, 2009), p. 127.
- ³⁵K. A. Gschneidner, Jr., Y. Mudryk, A. O. Tsokol, and V. K. Pecharsky, in *Proceedings of the 21st International Cryogenic Engineering Conference, Praha Czech Republic, 2007*, edited by G. G. Bagger (Institut International du Froid, Paris, 2007), Vol. 1, p. 621.
- ³⁶H. Yamada, *Phys. Rev. B* **47**, 11211 (1993).
- ³⁷M. Shimizu and A. Katsuki, *Phys. Lett.* **8**, 7 (1964).
- ³⁸J. D. Moore, G. K. Perkins, Y. Bugoslavsky, L. F. Cohen, M. K. Chattopadhyay, S. B. Roy, P. Chaddah, K. A. Gschneidner, Jr., and V. K. Pecharsky, *Phys. Rev. B* **73**, 144426 (2006).
- ³⁹J. D. Moore, G. K. Perkins, Y. Bugoslavsky, M. K. Chattopadhyay, S. B. Roy, P. Chaddah, V. K. Pecharsky, K. A. Gschneidner, Jr., and L. F. Cohen, *Appl. Phys. Lett.* **88**, 072501 (2006).
- ⁴⁰L. Jia, J. R. Sun, H. W. Zhang, F. X. Hu, C. Dong, and B. G. Shen, *J. Phys.: Condens. Matter* **18**, 9999 (2006).
- ⁴¹A. del Moral and D. Melville, *J. Phys. F* **5**, 1767 (1975).